HAL
open science

Strong reorganization of multi-domain microbial networks associated with primary producers sedimentation from oxic to anoxic conditions in an hypersaline lake

Arthur Escalas, Marc Troussellier, Delphine Melayah, Maxime Bruto, Nicolas Sébastien, Cécile Bernard, Magali Ader, Christophe Leboulanger, Hélène Agogué, Mylène Hugoni

To cite this version:

Arthur Escalas, Marc Troussellier, Delphine Melayah, Maxime Bruto, Nicolas Sébastien, et al.. Strong reorganization of multi-domain microbial networks associated with primary producers sedimentation from oxic to anoxic conditions in an hypersaline lake. FEMS Microbiology Ecology, 2022, 97 (12), pp.fiab163. 10.1093/femsec/fiab163 . hal-03443150

HAL Id: hal-03443150

https://hal.science/hal-03443150v1

Submitted on 23 Nov 2021

HAL is a multi-disciplinary open access archive for the deposit and dissemination of scientific research documents, whether they are published or not. The documents may come from teaching and research institutions in France or abroad, or from public or private research centers.

L'archive ouverte pluridisciplinaire **HAL**, est destinée au dépôt et à la diffusion de documents scientifiques de niveau recherche, publiés ou non, émanant des établissements d'enseignement et de recherche français ou étrangers, des laboratoires publics ou privés.

Strong reorganization of multi-domain microbial networks associated with primary producers sedimentation from oxic to anoxic conditions in an hypersaline lake

Escalas Arthur[1], Troussellier Marc[1], Melayah Delphine[2], Bruto Maxime[3], Nicolas Sébastien[2], Bernard Cécile[4], Ader Magali[5], Leboulanger Christophe[1], Agogué Hélène[6], Hugoni Mylène[2,7]

[1] MARBEC, Université de Montpellier, CNRS, IRD, IFREMER, Place Eugène Bataillon, Case 093, 34 095 Montpellier Cedex 5, France.
[2] Université de Lyon, Université Claude Bernard Lyon 1, CNRS, INRAE, VetAgro Sup, UMR Ecologie Microbienne, F-69622 Villeurbanne, France
[3] Université de Lyon, Université Lyon 1, CNRS, UMR5558, Laboratoire de Biométrie et Biologie Évolutive, 43 bd du 11 novembre 1918, 69622 Villeurbanne, France
[4] UMR 7245 MCAM, Muséum National d'Histoire Naturelle – CNRS, CP 39, 75005 Paris, France
[5] Université de Paris, Institut de physique du globe de Paris, CNRS, 75005 Paris, France
[6] Littoral Environnement et Sociétés (LIENSs) UMR 7266 CNRS –La Rochelle Université, 17000 La Rochelle, France
[7] Institut Universitaire de France (IUF)

ABSTRACT

Understanding the role of microbial interactions in the functioning of natural systems is often impaired by the levels of complexity they encompass. In this study, we used the relative simplicity of an hypersaline crater lake hosting only microbial organisms (Dziani Dzaha) to provide a detailed analysis of the microbial networks including the three domains of life. We identified two main ecological zones, one euphotic and oxic zone in surface, where two phytoplanktonic organisms produce a very high biomass, and one aphotic and anoxic deeper zone, where this biomass slowly sinks and undergoes anaerobic degradation. We highlighted strong differences in the structure of microbial communities from the two zones and between the microbial consortia associated with the two primary producers. Primary producers sedimentation was associated with a major reorganization of the microbial network at several levels: global properties, modules composition, nodes and links characteristics. We evidenced the potential dependency of Woesearchaeota to the primary producers' exudates in the surface zone, and their disappearance in the deeper anoxic zone, along with the restructuration of the networks in the anoxic zone toward the decomposition of the organic matter. Altogether, we provided an in-depth analysis of microbial association network and highlighted putative changes in microbial interactions supporting the functioning of the two ecological zones in this unique ecosystem.

Keywords: Archaea, Bacteria, Picoeukaryota, hypersaline ecosystem, microbial association network, *Arthrospira fusiformis, Picocystis salinarum*

INTRODUCTION

The functioning of ecological systems depends on a synergy of interacting organisms (Anantharaman *et al.* 2016; Hug and Co 2018). However, the levels of complexity in most natural systems and the communities they host make understanding the role of these interactions in the functioning of the system a daunting task. This is particularly true in microbial systems, which host thousands of species and where interactions are difficult to assess owing to the microscopic nature of the partners involved. In addition, microorganisms not only interact with each other but also with their predators, whether these are micro- (*e.g.* zooplankton, protozoa) or nanoscopic (*i.e.* phages), along with macro-organisms and their associated microbiomes (Troussellier *et al.* 2017). Such biological complexity is almost always associated with environmental variability, which modifies the composition of communities, and thus the interactions between their members, across spatial and temporal scales (Sunagawa *et al.* 2015; Bahram *et al.* 2018). Altogether, these various levels of complexity and variability limit our capacity to characterize, describe and ultimately understand the role of biological interactions in the functioning of natural systems. Nonetheless, some ecosystems present lower biological diversity and more stable environmental conditions, facilitating the study of the communities they host and the interactions between organisms. These include for instance aquatic ecosystems with extreme physico-chemical conditions such as hypersaline lacustrine ecosystems (Ventosa *et al.* 2015), which typically host a lower richness and diversity of organisms than other types of lakes and present less variable environmental conditions.

The recently characterized Lake Dziani Dzaha (Leboulanger *et al.* 2017) exhibits particularly stable geochemical and biological characteristics, and constitutes a modern analog of Precambrian ecosystems (Cadeau *et al.* 2020). This tropical thalassohaline crater lake is characterized by an important methane production (Cadeau *et al.* 2020; Sarazin *et al.* 2020) and contains only microbial organisms. It is characterized by extreme geochemical characteristics (salinity exceeds 60 psu, periodically high H_2S/HS^- concentrations, pH is higher than 9) along with the presence of at least two contrasted environments. An oxic layer, in surface, allowing autotrophic metabolisms, where a very high and stable biomass is produced ($mean_{2014\text{-}2015} = 652 \pm 179$ µg chlorophyll a.L^{-1}), mostly by two co-dominant photosynthetic organisms that exhibit complementary functional traits (Bernard *et al.* 2019), the cyanobacteria *Arthrospira fusiformis* and the picoeukaryote *Picocystis salinarum* (Chlorophyta, Cellamare *et al.*, 2018). Beside these two dominant taxa, the lake hosts bacterial, archaeal and eukaryotic communities of low diversity (Hugoni *et al.* 2018). In the deeper layers of the lake, *i.e.* below 2 m depth, there is no light nor oxygen all year round. A halocline periodically develops at around 2 m depth, mostly due to a density contrast induced by the abundant rainfalls of the rainy season. When it is in place, the concentration of H_2S/HS^- in the deep layers is high ($mean_{2014\text{-}2015} = 3052 \pm 1963$ µmol.L^{-1}). In this anoxic layer the primary producers decrease drastically in abundance while

still maintaining high abundances (*i.e.* 10^5-10^6 cells.mL^{-1}), and the bacterial and archaeal communities change along the depth profile (Hugoni *et al.* 2018). This water column is structured around the two dominant phytoplanktonic taxa (Leboulanger *et al.* 2017; Hugoni *et al.* 2018; Bernard *et al.* 2019). In the oxic surface layer, they constitute the point of entrance of the energy in the system and are expected to redistribute this energy to the whole microbial consortium in the form of secondary metabolites (Seymour *et al.* 2017). In the anoxic and light-depleted layer, the photosynthetic biomass is also the main source of energy and is anaerobically decomposed by heterotrophic prokaryotes. Consequently, the structure of the microbial assemblages and the interactions between organisms are of particular interest to better understand this atypical system and further, owing to its analogies with some Precambrian environments, to ultimately gain insights into their functioning.

During the last decade, association networks have gained a lot of interest in microbial ecology and their use for deciphering potential microbial interactions is now widespread (Faust *et al.* 2015; Röttjers and Faust 2018; Delmas *et al.* 2019; Faust 2021). This appeal for network approaches comes from their ability to synthesize in a single object (*i.e.* a graph), the amount of information that is contained in dozens or hundreds of microbial community profiles, each of them being composed of thousands of features (*e.g.* OTUs, ASVs, genes). However, most studies report only the analyses of global network properties (*e.g.* number of nodes or links, diameter, centralized metrics) and there are few studies that dare to dive into the complexity of the graph objects to provide deeper analyses of their structure. Indeed, networks are organized into different structural levels (network, modules, nodes and links) that complement each other and could provide deeper insights about the studied system if considered simultaneously (Niquil *et al.* 2020). Nodes identity and associations with each other provide information on their putative interactions, modules are groups of taxa closely associated that could correspond to functional groups with similar or complementary capabilities, and global network characteristic represent the system as a whole (Karimi *et al.* 2017; Pellissier *et al.* 2018; Delmas *et al.* 2019). In this study, we analyzed the attributes of microbial association networks from the two main ecological zones of the Dziani Dzaha lake (*i.e.* oxic and anoxic) at four structural levels of resolution (network, module, nodes, links), in order to better understand the linkages between network structure, interactions between organisms and the functioning of microbial communities in these zones.

In the present work, we aimed at understanding the associations between microorganisms from the three domains of life in the Dziani Dzaha lake to understand in greater details the functioning of this exceptional and unique ecosystem, hopefully also shedding light on Precambrian ecosystems. We hypothesized that the structure of the microbial assemblages and the interactions between the organisms surrounding the dominant taxa (the prokaryote *Arthrospira fusiformis* and the picoeukaryote *Picocystis salinarum*), will change between zones, but this remains to be tested. To achieve our purpose, we used data from a metabarcoding study of the three domains of life and applied a statistical network approach to

characterize the associations between microorganisms and the structure of microbial networks in the different ecological zones of the lake.

MATERIAL AND METHODS

Study site, sampling, and environmental parameters

The Dziani Dzaha lake is a volcanic crater lake located on the Mayotte Island (Western Indian Ocean), that is characterized by an important salinity (ranging from 34 to 71 psu), a high alkalinity (0.23 $mol.L^{-1}$) and a permanent green color due to high primary production. Water samples were collected along a depth profile located at the deepest point of the lake (0m, 1m, 2.5m, 5m, 11m, 15m and 17m depth), using a horizontal 1.2L Niskin bottle. Sampling campaigns occurred at end of both rainy (April) and dry (October-November) season, over two consecutive years (2014 and 2015). Vertical profiles for pH, dissolved O_2, temperature and conductivity were taken using either a MPP350 probe connected to a Multi 350i data logger (WTW GmbH) or a YSI 6600 probe. Salinity was calculated from conductivity and temperature measures. The concentrations of soluble sulfide (ΣS(-II), hereafter referred to H_2S/HS^-), ammonium and ammonia (∑N(-III); NH_4/NH_3), and soluble-reactive phosphorus (SRP; PO_4^{3-}) were determined by colorimetry in the field-lab using Aqualytic SpectroDirect spectrophotometer and Merck reagents kits. The concentration of Chla was analyzed after extraction using 96% ethanol by ultra-sonication in an ice bath for 30″, and further extraction was allowed overnight at 4 °C in dark. The extract was filtered, and the filtrate was analyzed spectrophotometrically at 400–750 nm. The concentration of Chla was calculated according to Camacho *et al.* (2009).

Delineation of ecological zones

To analyze the structure of association networks in the different ecological zones observed in the Lake Dziani Dzaha, the first step was to delineate these zones. To do so, we used six variables describing the physico-chemistry of the water column (temperature, pH, percentage of oxygen saturation, salinity, redox potential (Eh), H_2S/HS^- concentration) and one biological variable (total chlorophyll a concentration). These data were scaled to account for their differences in range and absolute values (*scale* function in R) and we computed Euclidean distance between samples. Then, we applied a kmeans classification approach using the *NbClust* package (Charrad *et al.* 2014) to determine the optimal number of groups based on a consensus estimated across 30 different indices evaluating the quality of the partition of samples into groups. Visualization of samples clustering was done using a hierarchical classification based on the Ward clustering algorithm. Differences between the identified ecological zones in terms of environmental parameters were tested using Wilcoxon rank sum test and p-values were adjusted using the Bonferroni correction.

144

145 **DNA extraction, Illumina sequencing and sequence processing**

146 Details regarding methodological procedures were described in Hugoni *et al.* (2018). Briefly, total-
147 to-3µm and 3-to-0.2µm fractions of water samples were collected through successive filtration on 3 µm and
148 0.2 µm filters. DNA was extracted using the Power Water DNA isolation kit (MoBio Laboratories).
149 Amplicons libraries were produced in triplicate using the universal bacterial primers 357F (Schuurman *et al.*
150 2004) and 926R (Walters *et al.* 2016), archaeal 519F and 915R (Hugoni *et al.* 2015) and eukaryotic 515F
151 (Caporaso *et al.* 2011) and 951R (Hugoni *et al.* 2018). Sequencing was done on an Illumina HiSeq 2500
152 system (GATC Biotech, Konstanz, Germany). Paired-end reads from both 3µm and 0.2µm filters were
153 pooled. Trimming, clustering and chimeric sequences removing was performed using the FROGS pipeline
154 (Escudié *et al.* 2018). To allow sample comparisons, bacterial, archaeal and eukaryotic datasets were
155 randomly resampled to 124,779, 37,529 and 36,840 sequences, respectively.

156

157 **Analyze of composition and structure of microbial communities**

158 Microbial communities from the identified ecological zones were compared using PERMANOVA
159 (Anderson 2001) as implemented in the R package *vegan* (function *adonis*, Oksanen *et al.*, 2016).
160 Differences in community composition were tested using Jaccard dissimilarity and differences in structure
161 were tested using Bray-Curtis dissimilarity. This was done for the three domains of life combined and
162 separately for each of them. The OTUs that contributed the most to differences in structures between zones
163 were subsequently identified using similarity percentage (SIMPER) analysis (function *simper* in the R
164 package *vegan*).

165

166 **Construction and characterization of association networks**

167 Microbial association networks for each community were constructed using SParse InversE
168 Covariance Estimation for Ecological Association Inference (Kurtz *et al.* 2015), as implemented in the R
169 package *SpiecEasi* (Kurtz *et al.* 2019). This approach allows the combination of independent compositions
170 matrices generated during separate sequencing run and is thus well suited for cross-domain studies (Tipton *et*
171 *al.* 2018). We followed the overall methodology described in Wagg *et al.* (2019). First, we used centered log-
172 ratio transformation (Gloor *et al.* 2017) on the OTUs tables from the three domains and combined them to
173 generate a meta-network using all available samples from each zone. The most parsimonious network
174 structure was identified for each zone using Stability Approach to Regularization Selection (StARS, Liu,
175 Roeder, & Wasserman, 2010) and the Meinshausen and Buhlmann algorithm. Second, sub-set networks for
176 each sample were extracted from the meta-network by selecting OTUs detected within the sample and these
177 were used to estimate networks characteristics at the sample level.

Association networks are composed of nodes (OTUs) that can be more or less connected to each other by edges (associations). Different but complementary insights about the studied system can be gained depending on whether one characterize the properties of the entire network, of its individual components (nodes or groups of nodes, *i.e.* modules) or their relationships (Niquil *et al.* 2020). Here we analyzed networks attributes at four levels of resolution (network, module, nodes, links) using the functions from the R package *igraph* (Csardi and Nepusz 2006).

First, the global characteristics of each sub-network were described using indices from the graph theory: number of nodes and edges, network density, average inter-nodes distance, centralized degree, betweenness and closeness, hub score (Pellissier *et al.* 2018; Delmas *et al.* 2019).

Second, we identified modules, *i.e.* groups of taxa that tend to have many associations between them and fewer outside of the group, and that potentially constitute a functional group because of their similar or complementary capabilities. There are many algorithms available to cluster taxa into modules and to reduce biases related to the choice of a single method we used six algorithms: edge betweenness, fast greedy, infomap, leading eigen vector, Louvain and walktrap. Then, we analyzed only the clustering from the algorithm that provided a number of modules within each zone comparable to the average estimated across all methods. Then, we compared the sizes and taxonomic composition of modules from the two zones.

Third, we computed centrality indices at the node level (degree, betweenness, closeness and hub score) and identified central and peripheral nodes as those whose average rank across indices felt within the first and tenth decile. Then, we compared taxonomic composition of central and peripheral nodes from the two zones.

Fourth, we identified the proportion of positive and negative links in different zones, the links that were maintained between zones along with the identity of the nodes associated with *Arthrospira fusiformis* and *Picocystis salinarum*.

Phylogenetic analyses of the Dziani Dzaha microbial communities

Representative OTUs sequences were compared with the SILVA database v 138.1 (Kim *et al.* 2019) using BlastN (Camacho *et al.* 2009) to identify the percentage of similarity between the queried sequences and their top hits. To assess sequences commonness, the distribution of their percentage identity was fitted with a normal distributions by using a maximum-likelihood method implemented in the PAST program (Hammer, Harper and Ryan 2001). This approach allowed us to define sequences as known (>95% identity to the SILVA database), poorly characterized (80-95%) or unknown (<80%).

RESULTS

Delineation of two strikingly different ecological zones in the lake

The kmeans classification approach suggested that the best grouping of samples based on their physico-chemical characteristics was in two clusters, one containing 16 samples and the other 12 (Figure 1). Overall, the samples were clustered according to depth (Figure 1-A). One cluster contained all the surface samples (*i.e.* depth from 0m to2.5m) and two deeper samples (5m and 11m, Figure 1-B). The other contained all the samples taken at 5m depth and below, plus two samples from 2.5m. Overall, the depth of clusters separation corresponded well with the halo/chemo-cline observed periodically in the lake at the end of rainy seasons and below which reduced species (including H_2S/HS^- and NH_4^+/ NH_3) accumulated. At the end of dry seasons although the halocline was not present and the concentration of reduced species remained quite low, bottom waters remained anoxic below 2 m depth. The surface samples exhibited significantly higher values in redox potential (Eh) and chlorophyll-a concentration while the bottom samples exhibited higher values in salinity and periodically higher concentrations of H_2S/HS^- (Table 1, Wilcoxon rank sum test, p-values < 0.05 with Bonferroni correction). The two groups of samples thus correspond well to two contrasted ecological zones. Hereafter, the oxic and euphotic zone will be termed “surface” while the deeper anoxic and aphotic zone will be termed “bottom”. This bottom layer could itself be separated in two sub-zones, alternating with time, depending on their concentration of reduced species which depends on the presence or absence of halocline. But our sample size was too low to allow a meaningful statistical characterization of the two sub-zones.

Similarity of Dziani Dzaha OTUs with reference databases

Overall, the Dziani Dzaha OTUs showed a little degree of similarity with the SILVA database, but this depended on the domain and phylum considered (Figures S1-S2-S3). We found that a third of bacterial (36%) and eukaryotic (34%) OTUs could be considered as well known (>95% sequence similarity), while this proportion dropped to 23% for archaeal OTUs. For Bacteria, 61% of OTUs were poorly characterized (80-95% similarity) and only 3% were considered as unknown (<80%). The proportion of unknown OTUs was much greater in Archaea (15% including a large proportion of Woesearchaeota and Euryarchaeota from the MEG class) and Eukaryota (44%, including almost all the Stramenopiles and all the Jakobida).

Structure of microbial communities in the two zones

The total and average OTUs richness were lower in the surface zone (n = 410 and 281±36, on average) compared with the bottom one (n = 427 and 317±30 on average, t.test p-value < 0.05 for the average richness). A total of 399 OTUs were shared between the two zones, which represented 91% of all the observed OTUs.

The microbial communities from the two environmental zones presented significantly different composition and structure (PERMANOVA, p-value < 0.05). This was confirmed for the multi-domain communities and for each domain separately (Table 2). The composition of bacterial communities differed the most, followed by archaeal and picoeukaryotic communities, as shown by the decreasing F values and R^2 of the PERMANOVA models. Differences were even stronger when considering OTUs abundance, as supported by higher F values of the PERMANOVA models. We identified 18 OTUs whose cumulative contribution represented 70% of the differences in structure between the microbial communities from the two zones (SIMPER analysis, Table S1). These included 9 bacterial, 7 archaeal and 2 eukaryotic OTUs. The highest bacterial contributor was by far the cyanobacteria *A. fusiformis*, followed by the Firmicutes (n = 4) and the Bacteroidetes (n = 3). Archaea corresponded mostly to Woesearchaeota (n = 4) and the methanogen group WSA2 (n = 2), while the highest picoeukaryotic contributors were the picophytoplankton *Picocystis* and the protist *Jakoba libera*.

Global characteristics of association networks

The networks from the two zones differed significantly regarding most of the global network properties tested (Figure 2 and S4, Table 3). The networks from the surface zone had a significantly lower number of nodes (272 *vs.* 310) and edges (790 *vs.* 1099), which were associated with a longer network diameter (maximum path length), a lower density and longer distance between nodes (*i.e.* average number of steps from one node to another). Centralized degree and hub score were lower in the surface zone.

Composition of network modules

The surface zone tends to have a higher number of modules across all clustering algorithms, but this was not significant (16.2±10.6 and 12.2±7.4 for the surface and bottom zones, respectively, Wilcoxon test, p-value = 0.377). Hereafter, we present only the results for the walktrap algorithm as the number of identified modules (13 and 10 for surface and bottom zones, respectively) reflects the average value estimated across all algorithms (Table S2). In the surface zone, near half of the modules (7/13) included OTUs from the three domains of life against less than a third (3/11) in the bottom zone. We observed one module composed of Archaea only in each zone (S_6 and B_7, Figure 3), and there were two modules composed of Bacteria only in the bottom zone (B_5 and B_9).

In both zones, the two dominant phytoplanktonic species belonged to separate modules (S_11 and B_9 for *A. fusiformis* and S_5 and B_8 for *P. salinarum* in surface and bottom zones, respectively) and these modules represented most of the total number of sequences in both zones (Figure 3).

282 *A. fusiformis* surface module (S_11) was composed of 22 OTUs belonging to three domains and 10
283 phyla. Firmicutes were the most represented phylum (5 OTUs), followed by Woesearchaeota (4),
284 Bacteroidetes (3), Euryarchaeota (3) and Proteobacteria (2). The number of OTUs within *A. fusiformis*
285 modules increased from 22 in surface to 36 in the bottom zone (module B_9, +64%). This was associated
286 with a high dissimilarity in the composition and structure of the modules between zones, with dissimilarity
287 ranging from 0.92 to 1 at the OTU level (Table S3). Changes in composition corresponded to the
288 disappearance of all the archaeal (-8) and eukaryotic (-1, *Nitzschia* sp.) OTUs, which were replaced by
289 Bacteria from the Firmicutes (+9), Bacteroidetes (+6), Proteobacteria (+4), Elusimicrobia (+2), along with
290 Actinobacteria and Synergisetes (+1 each).
291 *P. salinarum* surface module (S_5) was by far the one with the highest number of OTUs (n = 115),
292 which belonged to three domains and 27 phyla. Again, the Firmicutes were the most diverse phylum (27
293 OTUs), followed by Woesearchaeota (18), Bacteroidetes (11), Proteobacteria (11), Actinobacteria (7) and
294 Euryarchaeota (7). Contrarily to *A. fusiformis*, the number of OTUs within *P. salinarum* modules decreased
295 from the 115 in surface to 64 in the bottom zone (B_8, -44%). Here again this was associated with a very
296 high dissimilarity in module composition and structure between zones, with dissimilarity ranging from 0.8 to
297 0.94 at the OTU level (Table S3). The diversity of Archaea dropped sharply from the surface to the bottom
298 zone (-28 OTUs), with a notable loss of Woesearchaeota (-13) and Euryarchaeota (-6). Bacterial richness also
299 decreased (-23 OTUs), with loss of Clostridiales (-8), Bacteroidia (-5) and Alphaproteobacteria (-8).
300 Interestingly, while the number of picoeukaryotic OTUs remained stable (10) there was a strong turnover in
301 their composition (> 0.75 and > 0.8 at the Order and OTU levels, respectively), with the replacement of
302 Ascomycota (3 OTUs), Basidiomycota and Ciliophora (1 each) by the genus *Ancyromonas* (3 OTUs),
303 *Jakoba* (3 OTUs) and *Suigetsumonas* (1).
304
305
306 **Characteristics of network nodes**
307 The node-level centrality indices differed between zones in terms of degree, closeness, and hub score
308 (Wilcoxon test, p-values < 0.05), with the first two being higher in the bottom zone (Figure S5). We observed
309 that the relationships between the average node rank across indices and its standard deviation exhibited a bell
310 shape (Figure S6), meaning that the most central and most peripheral nodes were the same whatever the
311 index and that the centrality of many nodes in the network depended on the selected index. Hereafter, we
312 analyze in detail the taxonomy of the most central and peripheral nodes, identified as those whose average
313 rank across indices fell within the first and tenth decile (n = 36 and 37 in surface and bottom zones,
314 respectively).
315 Picoeukaryotes and Archaea represent around 10% and 30% of the total number of OTUs,
316 respectively. However, Picoeukaryotes appeared over-represented in the central nodes, as they represented

317 17% and 14% of the central nodes in the surface and bottom zones, respectively (Figure 4). Contrarily,
318 Archaea were over-represented in peripheral nodes, as they represented >50% of them in both zones. In
319 addition, we observed a strong turnover in the taxonomic composition of both central and peripheral nodes
320 (Jaccard dissimilarity = 0.92), with only 5 out of 36 OTUs being central in both zones. These included 4
321 Bacteria (2 Clostridiales, 1 Anaerolinae and 1 Deltaproteobacteria) and one WSA2 Archaea. Among the taxa
322 that lost their central position in the network in the bottom zone, we identified Stramenopiles, Bacteroidetes,
323 Woesearchaeota, Acidobacteria and the MEG Euryarchaeota, while the taxa that became central included
324 mainly Jakobida, Firmicutes and Proteobacteria (Table S4).
325 The two dominant taxa were not identified as peripheral nor central nodes but several members of
326 their modules were identified as central nodes. In surface, 26 of the 36 central OTUs (72%) originated from
327 *P. salinarum* module (S_5), including notably five Firmicutes, four Woesearchaeota and four Bacteroidetes,
328 while only two were from *A. fusiformis* module (S_11). In the bottom zone, the dominant taxa modules were
329 less represented in central nodes (4 and 9 for *A. fusiformis* and *P. salinarum*, respectively), and these OTUs
330 corresponded mostly to Firmicutes (n = 2 and 4), with also one Jakobida OTUs from *P. Salinarum* module.
331
332
333 **Characteristics of network links**
334 Overall, the proportion of positive links was lower in the surface zone (54% *vs.* 60%) but their
335 absolute strength was higher (0.15 *vs.* 0.13). We observed that seven out of the ten strongest positive links
336 involved two archaeal OTUs and six of them involved pairs of OTUs from the same class. Among these
337 strong links, Woesearchaeota and WSA2 were only involved in links from the surface while Euryarchaeota
338 (Methanomicrobia and Thermoplasmata) were found in strong links from both zones. We found 44 links that
339 were conserved in both zones, which represents less than 2% of the total number of links, and they were
340 positive for a wide majority (84%, 37/44). These conserved links involved 79 OTUs, with only 9 OTUs
341 being involved in more than one link. These included three Woesearchaeota and one Euryarchaeota, two
342 Clostridiales and one Bacteroidetes, along with the Eukaryote *Planomonas micra*.
343 The dominant taxa exhibited a similar number of linkages but the proportion of positive links was
344 much higher in *P. salinarum* (57 and 86%, in surface and bottom zone) than *A. fusiformis* (43 an 22%). The
345 taxonomic identity of the OTUs directly linked with dominant taxa differs greatly between zones and no link
346 was maintained in both zones (Table 4).
347
348
349
350
351

352 **DISCUSSION**

353

354 **The two contrasted environmental zones of the water column**

355 Samples clustering based on their physico-chemical characteristics confirm previous observations of
356 the existence of two ecological zones (Leboulanger *et al.* 2017), one oxic and euphotic layer in surface
357 dominated by photosynthetic processes (0-2.5m depth), and one anoxic and aphotic zone at greater depth (2-
358 17m). The depth of zone separation corresponded well with the halo/chemo-cline periodically observed in
359 the lake in the form of large changes in salinity, redox potential, H_2S/HS^- and chlorophyll *a* concentration.
360 The periodical stratification of the lake that results from rainfalls was shown to be associated with the
361 presence of a third ecological zone in the deepest part of the lake (*i.e.* below 14m) where the concentrations
362 of H_2S/HS^- are the highest (Sarazin *et al.* 2020). However, the statistical approach used here to delineate
363 ecological zones was not able to separate deep samples from the stratified period from the others deep
364 samples. Nonetheless, our results validate previous studies on Dziani Dzaha lake suggesting that the two
365 main zones of the lake represent totally different environments from the microbial point of view.

366

367 **Reorganization of microbial communities and networks from one zone to the other**

368 Despite 91% of shared OTUs between zones, the distribution of their abundances strongly differed
369 between them, suggesting a reorganization of the microbial communities. This included notably changes in
370 abundances within the bacterial Firmicutes and Bacteroidetes phyla, along with the archaeal Woesearchaeota
371 phylum and the methanogen group WSA2. In addition, we observed slightly higher total (+4%) and average
372 (+13%) number of OTUs in the bottom zone.

373 These differences in community structure were associated with modifications of the structure of
374 association networks at several levels of their organization. Global network properties suggested that the
375 network increased in complexity in the bottom zone, with more taxa being involved and more connections
376 between them, and became more compact, as the inter node distance shortened and its density increased. In
377 addition, the associations between taxa were weaker and more positive in the bottom zone. Overall, these
378 results provide a picture of a more balanced network in the bottom zone, with a high number of inter-taxa
379 associations, most likely corresponding to cross-feeding and metabolic handoff (Anantharaman *et al.* 2016;
380 Hug and Co 2018), in order to anaerobically degrade the carbon provided by the lysis of sinking cells from
381 the primary producers (10% of the cells remaining in the bottom zone, (Bernard *et al.* 2019). It was
382 previously shown that strong dominance by cyanobacteria in freshwater plankton communities, as observed
383 here in the surface zone, resulted in unbalanced networks and a higher proportion of negative associations
384 than when dominance is less marked (Escalas *et al.* 2019).

385 We observed a very strong reorganization of the components of Dziani Dzaha lake microbial
386 networks from the surface to the bottom zone, with less than 2% of the links (n = 44) that were conserved in

387 both zones. In other terms, the associations between microorganisms changed from one zone to the other to
388 support the different metabolic processes occurring in each zone. Here, we can hypothesize that the surface
389 microbial network is organized around the metabolic byproducts released by the two primary producers
390 while the bottom network is organized around the decomposition of their biomass.
391 In addition, the position of taxa within the network changed between zones, as 86% of the central
392 OTUs in the surface zone were not central any more in the bottom zone. Only five OTUs were found to be
393 central within both zones. These included two Firmicutes from the Clostridia class: one was a
394 Halanaerobiale, a group of anaerobic and halophilic organisms presenting a great metabolic diversity
395 including the ability to ferment carbohydrates and to grow chemolithoautotrophically on hydrogen and
396 elemental sulfur, and the other a Peptostreptococcaceae, recognized as hyper-ammonia-producing bacteria
397 (Gomes Carvalho Alves *et al.* 2021). The remaining two bacterial OTUs included a Bdellovibrionaceae
398 (Deltaproteobacteria), which are intraperiplasmic predator that prey upon a variety of plant-pathogenic and
399 growth-enhancing Bacteria (Jurkevitch *et al.* 2000), and an Anaerolineaceae (Chloroflexi), a family found
400 in sulfidic environments and known for their capacity to degrade hydrocarbons and participate in
401 syntrophic CH_4 production (Liang *et al.* 2015). The last OTU was an archaeal WSA2, a group of
402 methanogens that may bridge the carbon and sulfur cycles in eutrophic methanogenic environments (Nobu
403 *et al.* 2016).
404 The number and composition of network modules also changed from one zone to the other. The total
405 number of modules decreased (13 to 10), with notably a sharp drop in the number of modules composed of
406 taxa from the three domains of life (7 to 3), and the presence of two modules composed of Bacteria only in
407 the bottom zone. The lower number of modules in the bottom zone could be explained by its more
408 homogeneous environmental conditions (*e.g.* Mühlenbruch *et al.*, 2018; Kharbush *et al.*, 2020) which could
409 limit our ability to estimate co-variations of abundance between microorganisms, a prerequisite for the
410 identification of modules. It is worth noting that ecological significance of network modules is not yet clearly
411 defined nor understood (Faust 2021), and could correspond to groups of organisms (i) with similar
412 environmental preferences (*e.g.* anaerobic Firmicutes), (ii) with complementary functional traits and that
413 cooperate to realize a particular step in the nutrient cycle (*e.g.* fermentation of polysaccharides by
414 Clostridiales), (iii) that consume each other and constitute a trophic network (*e.g.* Jakobida predation on
415 bacteria) or (iv) that interact in a parasitic, commensal or symbiotic manner (*e.g.* associations between
416 Woesearchaeota and primary producers).
417
418 **Focus on microbial modules associated with the dominant primary producers**
419 We found that the two dominant primary producers, the prokaryote *Arthrospira fusiformis*
420 (Cyanobacteria, Oscillatoriales) and the picoeukaryote *Picocystis salinarum* (Chlorophyta, Prasinophyceae),
421 were members of distinct modules and thus were associated with different microbial consortia. The first

422 striking result is that the consortium associated with *P. salinarum* in the surface zone contained five times
423 more OTUs than the one of *A. fusiformis* (105 *vs.* 22). Hence, the number of OTUs associated to the much
424 smaller phytoplanktonic species was higher than the number of OTUs associated with the larger ones. This is
425 contradictory with the expectation that the number of microbial taxa associated with phytoplanktonic cells is
426 positively correlated with their size (Seymour *et al.* 2017). Regarding the taxonomic structure of these
427 consortia in the surface zone, we observed similarities in the archaeal communities, with notably
428 Woesearchaeota being dominant, but bacterial and picoeukaryotic communities differed greatly. It is well
429 known that several characteristics of phytoplanktonic taxa determine their associations with specific
430 procaryotic taxa (Goecke *et al.* 2013; Guedes *et al.* 2018; Jackrel *et al.* 2021). Hence, different hypotheses
431 can be proposed to explain the unexpected differences between the two phytoplanktonic species modules in
432 terms of OTUs number and taxonomic classification.
433
434 First, it could be related with the metabolic differences between the two dominant species, their
435 ability to secrete various type of organic molecules and thus to support different microbial consortia
436 (Grossart *et al.* 2005; Bagatini *et al.* 2014; Guedes *et al.* 2018). Indeed, in pelagic marine ecosystems,
437 phytoplankton constitute a source of a large diversity of organic molecules that influence heterotrophic
438 procaryotes, including substrates that support their growth (Fouilland *et al.*, 2014) but also signaling
439 molecules that determine synergetic or antagonist relationships among and with them (*e.g.* Amin *et al.* 2015;
440 Cirri and Pohnert 2019). High concentrations of dissolved organic carbon were reported in the euphotic layer
441 of the Dziani Dzaha lake (*i.e.* 3-9 mMol.L^{-1}, Sarazin *et al.* 2020), which likely result from the release of
442 various organic molecules by the large biomasses of the cyanobacteria *A. fusiformis* (600-700 µg Chla.L^{-1},
443 Bernard *et al.*, 2019).
444 However, the two phytoplanktonic dominant taxa differ in many ways regarding their potential for
445 exudates production, and particularly exopolysaccharides (EPS). EPS are generally composed of various
446 substances, such as proteins, polysaccharides, lipids, humic-like substances, DNA, lipopolysaccharides and
447 glycoprotein heteropolymers. EPS may be entirely released into the extracellular environment or may be
448 associated with the cell surface as sheaths, capsules or slime (Pereira *et al.* 2009).
449 Indeed, while *P. salinarum* appears unable to produce such polymers (Gaignard *et al.* 2019), the whole
450 *Arthrospira* genus is well known for its ability to produce EPS and was shown, in experimental conditions,
451 to produce the largest amounts with light and temperature levels similar to those of the euphotic layer of the
452 Dziani Dzaha lake (Trabelsi *et al.* 2009; Phélippé *et al.* 2019). Antibacterial properties have been reported for
453 cyanobacterial EPS (Xiao *et al.* 2018) and could explain the limited number of heterotrophic procaryotic
454 OTUs observed within *A. fusiformis* module. From a mechanical standpoint EPS act as a gel matrix which
455 can protect *Arthrospira* against bacterial colonization or other stressors and then reduce the number of taxa
456 able to move around the cyanobacteria surface. From a chemical standpoint, EPS are complex polymers that

457 only certain bacterial taxa are able to metabolize. Here, we found one Rhodobacteraceae and two ML635J-40
458 aquatic group OTUs in *A. fusiformis* module, and six Rhodobacteraceae, seven ML635J-40 aquatic group
459 and one Flavobacteria OTUs in *P. salinarum* module. The two bacterial groups are often associated with
460 oceanic phytoplankton blooms for their putative role in the degradation of EPS, the Flavobacteria class
461 (Bacteroidetes phylum) and the genus *Roseobacter* (Alphaproteobacteria from the Rhodobacteraceae family,
462 (Buchan *et al.* 2014). Flavobacteria are able to transform high molecular weight (HMW) compounds such as
463 EPS or transparent exopolymer particles (TEP) into low molecular weight (LMW) compounds (*e.g.* free
464 amino acids, sugars, mono- and dicarboxylic acids, (Buchan *et al.* 2014), while Roseobacter is considered as
465 mainly able to uptake and use the resulting LMW compounds (Taylor *et al.* 2014). This complementary
466 association might underlie the co-occurrence of these two bacterial groups already reported in several studies
467 (Pinhassi *et al.* 2004; Teeling *et al.* 2016). Another group of Bacteroidetes, the ML635J-40 aquatic group,
468 observed in the dominant organisms' modules might be related to the degradation of EPS. This group was
469 found to play a prominent role in the anaerobic digestion of *Arthrospira* in extreme alkaline conditions
470 (Nolla-Ardevol, Strous and Tegetmeyer 2015) and the authors report that their representative sequences were
471 classified as ML635J-40 using the SILVA database and as Flavobacteria using the RDP database. Thus, our
472 results suggest the involvement of these taxa in the breakdown of the substrates released by the
473 phytoplankton, and notably the EPS produced by *A. fusiformis*.
474 Less data is available on the biochemical composition and the kinds of molecules produced by the
475 picoeukaryote *P. salinarum*. Chemical analyses revealed that it contains a large number of different
476 carotenoids and that the sugar moieties of the cell wall matrix were mannose (68%), galactose (17%) and
477 glucose (5%) (Lewin *et al.* 2000), while the major fibrous component of its cell wall is polyarabinose. *P.*
478 *salinarum* contains a high proportion of lipids, especially when the cells are submitted to nitrogen limitation
479 (Tarazona Delgado *et al.* 2021), and strains isolated from Mono Lake synthesize a variety of fatty acids, with
480 palmitic acid (C_{16}) being the most abundant (Phillips *et al.* 2021).
481 Second, the unexpected difference in the number OTUs in the two phytoplanktonic species modules
482 could be a consequence of physical differences between them (Bernard *et al.* 2019). Indeed, with an average
483 biovolume of 10 μm^3 *P. salinarum* appears to belong to free living microbes, while *A. fusiformis* is on
484 average 23.5 times larger (235 μm^3). In addition to its smaller size, *P. salinarum* has a surface/volume ratio
485 (2.2) that is five time higher than the one of *A. fusiformis* (0.45). As a result of these two features, *P.*
486 *salinarum* is well mixed with free living microorganisms, which increases its chances of interacting with
487 them and could explain the higher number of OTUs observed in its module. A step further, *A. fusiformis* and
488 its surrounding EPS may be assimilated to the large size particles observed in marine ecosystems where
489 anoxic micro-zones can develop (Bianchi *et al.* 2018), which could explain the presence of Clostridiales in *A.*
490 *fusiformis* module. It is thus likely that around the circle of primary EPS degraders intimately associated to
491 *A. fusiformis* (*e.g.* Rhodobacteraceae, ML635J-40 aquatic group), many free-living OTUs are able to use the

492 different LMW compounds resulting from the degradation of these long polymers along with the substrates
493 produced by *P. salinarum*. Furthermore, the size differences between the two dominant organisms are
494 expected to impact they physical behavior within the system, and notably the way they sink from the oxic to
495 the anoxic part of the lake.
496
497
498 **Modifications of microbial corteges associated with the primary producers from the euphotic zone to**
499 **the aphotic and anoxic one**
500
501 Considering only the biovolume of the two phytoplanktonic species, one can expect that *A.*
502 *fusiformis* filaments will sink faster to the bottom zone than *P. salinarum* cells. To evaluate this hypothesis,
503 we estimated the sinking speed of each species by combining models relating the sinking speed of
504 phytoplanktonic cells with their volume and their morphometry (Durante *et al.* 2019), and using biovolume
505 measurements from Cellamare *et al.* (2018). Doing so, we estimated a sinking speed of 0.142 and 0.01
506 $m.day^{-1}$ for *A. fusiformis* filaments and *P. salinarum* cells, respectively. In other words, these organisms will
507 theoretically take near 120 and 1700 days to sink from the bottom of the surface of the lake down to the
508 bottom of the studied water column (18 m deep), respectively. These estimates do not account for the
509 viscosity of the water (which is expected to increase with the concentration of EPS), nor the fact that cells
510 have to cross several clines (thermal, haline and chemical) and that *A. fusiformis* have the capacity to modify
511 its buoyancy thanks to specialized cells. Nonetheless, the combination of higher biomass and faster sinking
512 rates should result in a higher flux of *A. fusiformis* cells from the oxic to the anoxic zone compared with *P.*
513 *salinarum*. However, estimations of these two species abundances using flow cytometry revealed that on
514 average 32% of the *P. salinarum* cells from the surface reached the bottom of the water column compared
515 with only 5% for *A. fusiformis* filaments (Bernard *et al.* 2019). Thus, if the rate of disappearance of
516 individuals of *A. fusiformis* and *P. salinarum* were identical, then individuals of the slower sinking species (*P.*
517 *salinarum*) would have to disappear more rapidly than those of the faster sinking species (*A. fusiformis*). Yet,
518 the opposite was observed. It is therefore likely that the survival of *P. salinarum* cells is much higher than
519 that of *A. fusiformis* filaments.
520 We observed strong modifications of the associations between the dominant organisms and other
521 members of the microbial assemblages from one zone to the other. The most striking result was the total
522 disappearance of the associations between Archaea and *A. fusiformis*, which notably included the loss of six
523 Woesearchaeota OTUs (four from the module and two with a direct link). These uncultivated Archaea are
524 ubiquitous in anoxic and saline ecosystems but very little is known about their ecology and metabolic
525 potential (Casamayor, Triadó-Margarit and Castañeda 2013). In addition, comparisons with reference
526 databases showed that Woesearchaeota from the Dziani Dzaha lake can be considered as totally unknown (<

527 80% of sequence similarity). Previous studies based on bioinformatics analyses highlighted their small
528 genome size while metabolic reconstructions support an anaerobic heterotrophic lifestyle with conspicuous
529 metabolic deficiencies (Castelle and Banfield 2018; Dombrowski *et al.* 2020). This incomplete metabolic
530 potency strongly suggests an obligate associative lifestyle with a dependency on other microbes for
531 metabolic complementarity and is in line with their association with the dominant taxa and potential reliance
532 on phytoplanktonic exudates or their by-products following degradation by other microbes. Recent studies
533 predicted the role of Woesearchaeota in carbon cycling, through syntrophic relationship with methanogens,
534 and an involvement in nitrogen and sulfur cycle in sulfur rich ecosystems (Liu *et al.* 2018; Liu, Wang and Gu
535 2021). Thus, we hypothesized that they could benefit from anoxic microenvironments provided by
536 phytoplanktonic phycospheres or by aggregates formed with methanogens (the later also explaining the
537 presence of WSA2 in the oxic zone). These lost Archaea were notably replaced by members of the bacterial
538 ML635J-40 aquatic group (six OTUs in bottom module and four direct links) that are known for their ability
539 to degrade dead phytoplanktonic cells and notably *Arthrospira* (Nolla-Ardevol, Strous and Tegetmeyer
540 2015). This turnover in the taxa associated with *A. fusiformis* clearly suggests a shift of this species role from
541 an active photosynthetic organisms that feeds dependent taxa (*e.g.* Woesearchaeota), to a substrate that is
542 degraded in anaerobic conditions by specialized taxa (*e.g.* Rhodobacteraceae, ML635J-40 aquatic group),
543 resulting into a myriad of organic matter types that might support the observed reorganization of microbial
544 networks.
545 Regarding the fate of *P. salinarum* in the bottom zone, it appears more likely that this organism is
546 able to maintain a certain level of activity or at least to survive for a longer period of time than *A. fusiformis*.
547 Although the ability of this picoeukaryotic species to survive at extremely low light level was already
548 reported, Phillips *et al.* (2021) were the first to question its *in situ* ecophysiology in the hypolimnion of the
549 Lake Mono, where light conditions are similar to those found in the Lake Dziani Dzaha, *i.e.* no or a very
550 limited amount of light. These authors reported transcripts of photosynthetic genes from deep water samples
551 and proposed a fast-sinking speed of *P. salinarum* cells (0.5-1 $m.day^{-1}$) to explain the presence of such
552 transcripts. Thus, these transcripts would be the result of the survival of fast sinking cells rather than an
553 active growing process (no light, no photosynthesis). This hypothesis cannot be retained in the Dziani Dzaha
554 lake considering the sinking speed estimated for *P. salinarum*. The alternative hypothesis proposed by
555 Phillips *et al.* (2021) was that the survival of *P. salinarum* in the deep hypolimnion of Lake Mono, and
556 potentially in the Lake Dziani Dzaha, could be the consequence of a shift from photosynthetic to
557 fermentative pathways, as demonstrated for other green algae (Catalanotti *et al.* 2013), allowing it to survive
558 in anoxic and aphotic waters. To our knowledge, this interesting feature has not been confirmed in the Lake
559 Dziani Dzaha. We also found various Picoeukaryotes (Ancyromonadida, Stramenopiles and Jakobida) within
560 *P. salinarum* module in the bottom zone, suggesting a potential predation on this species. However, the size

difference between *P. salinarum* (3µm) and these potential predators (<7µm) does not seem to validate this hypothesis and rather suggest a grazing pressure on its associated prokaryotes.

CONCLUSIONS

In this study, we described the associations between microorganisms from the three domains of life in a hypersaline and hyperalkaline crater lake, modern analog of Precambrian ecosystems. We showed that the Dziani Dzaha lake is characterized by two main ecological zones, one euphotic and oxic zone in surface where two co-dominant phytoplanktonic organisms with complementary traits produce a steady and very high biomass, and one aphotic and anoxic deeper zone where the sinking particles of primary producers, especially *A. fusiformis*, are degraded and support the microbial production of methane. We highlight differences in the microbial communities' structure between the two zones, associated with a major reorganization of the microbial networks. Notably, we showed the potential dependency of Woesearchaeota to the primary producers' exudates in the oxic zone along with the disappearance of this group in the deeper layers of the lake. In the anoxic zone, the microbial networks are restructured toward the decomposition of the organic matter through microbial reassociations and notably the higher importance of Bacteroidetes from the ML635J-40 aquatic group.

The very active productivity of Dziani Dzaha lake has been shown to remain stable over long time periods and has already inspired biomimetic technological development. Here, three groups of prokaryotes appeared particularly important in the microbial dynamics and association networks of this lake: Clostridiales, Bacteroidetes and Woesearchaeota. Unfortunately, representatives of these taxa from Dziani Dzaha lake showed very little similarity with reference databases and limited their taxonomic identification. This further highlighted the exceptional and unique aspect of this ecosystem, not only from a geochemical standpoint but also considering its biodiversity. The need for further studies on this ecosystem is even more pronounced as it is currently under the threat of strong perturbations including its possible disappearance due to the emergence of a submarine volcano associated with an intense seismic activity leading to the subsidence of the Mayotte archipelago. These could allow to test fundamental concepts in microbial ecology such as the resistance and resilience of microbial communities to environmental disturbances.

Although we identified some potential interactions between the primary producers and Woesearchaeota, such association are purely statistic and remain to be validated using analyses at finer scales, such as cell sorting of the phytoplanktonic cells followed by analyses of the microbial consortia directly attached to them (*i.e.* their phycosphere). A surprising result was that *A. fusiformis* was not identified as a central taxa in the networks despite being the main component of the microbial communities owing to its biomass. This highlight a potential limitation of the network approach due to the fact that the permanence of this species at high biomass did not allow the identification of co-variations with other taxa. As most of

microorganisms from the lake are not cultivated yet due to the difficulty to reproduce its harsh environmental conditions, the use of genome resolved metagenomics approaches should provide greater insights into the genomic abilities of these uncultivated microorganisms. Nonetheless, the relative "simplicity" of this system with the two contrasted ecological zones and a purely microbial and low diversity biocenose allowed us to provide a deep and multiscale analysis of the microbial networks (global properties, modules composition, nodes and links characteristics). Doing so, we were able to get a deeper understanding of this ecosystem functioning (synthesized in Box 1) and such approach should be further deployed in other microbial systems.

Funding

This work was granted by the Total Corporate Foundation (project DZAHA, grant number C001493) and the French National Research Agency (project DZIANI, ANR-13-BS06-0001).

Acknowledgements

The field permit was granted by the Conservatoire du Littoral et des Rivages Lacustres, Antenne Océan Indien, due to the fact that Dziani Dzaha lake is currently a protected water body with free public access but restricted activities, under the control of the French agency for littoral ecosystems conservation (http://www.conservatoire-du-littoral.fr/).

Conflicts of interest

The authors declare no conflict of interest related to this work.

BOX 1 – What did we learned from network analysis of Dziani Dzaha lake microbial communities ?

In this section, we present an interpreted synthesis of our results that translate the observed networks characteristics into biological and ecological insights. The main results are graphically synthesized in Figure 5.

First of all, we confirmed the presence of two ecologically contrasted zones in the Dziani Dzaha lake and the low diversity of its microbial communities. In addition, we found that the two zones shared 91% of the OTUs and mostly differed in terms of OTUs relative abundances, illustrating the Baas-Becking theory (De Wit and Bouvier 2006).

Then, we found that in the surface zone the two main primary producers *Arthrospira fusiformis* (Cyanobacteria) and *Picocystis salinarum* (Chlorophyta) were associated with different microbial consortia (*i.e.* modules and direct associations). As modules are often interpreted as putative functional groups (Faust 2021), the differences in the taxonomic composition of primary producers modules suggest that they might play a different functional role in the system. In addition, the number of OTUs was lower in *A. fusiformis* (n = 22) module than in *P. salinarum* (n = 115) one, and we hypothesize that this counterintuitive result considering the size difference between these two taxa (Seymour *et al.* 2017) was likely the result of their different lifestyle, with *A. fusiformis* constituting a large particle and *P. salinarum* being part of the free living community.

Taxa centrality within the network is often considered as an indicator of their importance within the system and higher influence on the realized functions (notion of hub or keystone taxa). Here, we were surprised that both primary producers were not central according to centrality metrics (*e.g.* degree, betweenness, hub score), but the majority of central OTUs in the surface network were part of *P. salinarum* module (72%). This suggests that the free living assemblage realizes the main biogeochemical processes in the surface zone, which likely correspond to syntrophic metabolic processes that transform organic substrates released by primary producers, into dissolved nutrients. Contrarily, OTUs from *A. fusiformis* module were not central, which might reflect their specialization toward a phycosphere associated lifestyle. In addition, Protozoa were found to be more central in the network than expected considering their number, which likely represents their role as predator of Bacteria and Archaea. Despite these differences in associations between the two primary producers, they were both associated with Woesearchaeota, which supports the fact that this group is known to depend on the release of organisms substrates by other taxa as a result of its reduced genomic repertoire.

In a second time, the cells produced in the surface zone sink in deeper layers of the lake, where they encounter anoxic, aphotic and H_2S/HS^- rich environmental conditions that results in the lysis and degradation of primary producers that decrease in abundance (especially *A. fusiformis*). The sinking speed

655 estimated for the two phytoplanktonic taxa were quite low, and this likely allowed the shift in their functional
656 role in the system, from harvester of solar energy in the surface layer and redistributors of organic molecules
657 to a diversified organic matter pool that fuel fermentative processes in the bottom zone. This was reflected in
658 the disappearance of association with Woesearchaeota and the replacement of this group by anaerobic
659 fermenter (*e.g.* Rhodobacteraceae, ML635J-40 aquatic group).
660
661 If we shift the focus from the primary producers to the whole network, we observed that the bottom
662 zone network contained more modules, which might indicate a higher diversity of functional groups that
663 occupy a wider diversity of ecological zones. The bottom network also appeared more complex, with more
664 OTUs, more connections between them, a higher density of links and a shorter distance between nodes
665 (number of steps to link any pair of OTUs). All these indices could be the sign of a higher interdependence of
666 microorganisms for the realization of the collective degradation of the different types of organic matters
667 resulting from the degradation of primary producers (mostly *A. fusiformis* and its EPS). Central nodes from
668 the bottom network were different from the surface ones, with notably the replacement of archaeal OTUs by
669 Firmicutes and Chloroflexi, which constitutes another sign of the reorganization of the network toward a
670 different functional state.
671
672
673
674
675
676
677
678
679
680
681
682
683
684
685
686
687
688
689

690

691

692 **REFERENCES**

693

694 Amin SA, Hmelo LR, Van Tol HM *et al.* Interaction and signaling between a cosmopolitan phytoplankton
695 and associated bacteria. *Nature* 2015;**522**:98–101.

696 Anantharaman K, Brown CT, Hug LA *et al.* Thousands of microbial genomes shed light on interconnected
697 biogeochemical processes in an aquifer system. *Nat Commun* 2016;**7**:1–11.

698 Anderson MJ. A new method for non-parametric multivariate analysis of variance. *Austral Ecol* 2001;**26**:32–
699 46.

700 Bagatini IL, Eiler A, Bertilsson S *et al.* Host-specificity and dynamics in bacterial communities associated
701 with bloom-forming freshwater phytoplankton. *PLoS One* 2014;**9**, DOI: 10.1371/journal.pone.0085950.

702 Bahram M, Hildebrand F, Forslund SK *et al.* Structure and function of the global topsoil microbiome. *Nature*
703 2018;**560**:233–7.

704 Bernard C, Escalas A, Villeriot N *et al.* Very Low Phytoplankton Diversity in a Tropical Saline-Alkaline
705 Lake, with Co-dominance of *Arthrospira fusiformis* (Cyanobacteria) and *Picocystis salinarum*
706 (Chlorophyta). *Microb Ecol* 2019;**78**, DOI: 10.1007/s00248-019-01332-8.

707 Bianchi D, Weber TS, Kiko R *et al.* Global niche of marine anaerobic metabolisms expanded by particle
708 microenvironments. *Nat Geosci* 2018:1–6.

709 Buchan A, LeCleir GR, Gulvik CA *et al.* Master recyclers: features and functions of bacteria associated with
710 phytoplankton blooms. *Nat Rev Microbiol* 2014;**12**:686–98.

711 Cadeau P, Jézéquel D, Leboulanger C *et al.* Carbon isotope evidence for large methane emissions to the
712 Proterozoic atmosphere. *Sci Rep* 2020;**10**, DOI: 10.1038/s41598-020-75100-x.

713 Camacho C, Coulouris G, Avagyan V *et al.* BLAST+: Architecture and applications. *BMC Bioinformatics*
714 2009;**10**:27–41.

715 Caporaso JG, Lauber CL, Walters WA *et al.* Global patterns of 16S rRNA diversity at a depth of millions of
716 sequences per sample. *Proc Natl Acad Sci* 2011;**108**:4516–22.

717 Casamayor EO, Triadó-Margarit X, Castañeda C. Microbial biodiversity in saline shallow lakes of the
718 Monegros Desert, Spain. *FEMS Microbiol Ecol* 2013;**85**:503–18.

719 Castelle CJ, Banfield JF. Major New Microbial Groups Expand Diversity and Alter our Understanding of the
720 Tree of Life. *Cell* 2018;**172**:1181–97.

721 Catalanotti C, Yang W, Posewitz MC *et al.* Fermentation metabolism and its evolution in algae. *Front Plant*
722 *Sci* 2013;**4**, DOI: 10.3389/fpls.2013.00150.

723 Cellamare M, Duval C, Drelin Y *et al.* Characterization of phototrophic microorganisms and description of
724 new cyanobacteria isolated from the saline-alkaline crater-lake Dziani Dzaha (Mayotte, Indian Ocean).
725 *FEMS Microbiol Ecol* 2018;**94**, DOI: 10.1093/femsec/fiy108.

Charrad M, Ghazzali N, Boiteau V *et al.* Nbclust: An R package for determining the relevant number of clusters in a data set. *J Stat Softw* 2014;**61**:1–36.

Cirri E, Pohnert G. Algae−bacteria interactions that balance the planktonic microbiome. *New Phytol* 2019;**223**:100–6.

Csardi G, Nepusz T. The igraph software package for complex network research. *InterJournal* 2006;**Complex Sy**:549–51.

Delmas E, Besson M, Brice MH *et al.* Analysing ecological networks of species interactions. *Biol Rev* 2019;**94**:16–36.

Dombrowski N, Williams TA, Sun J *et al.* Undinarchaeota illuminate DPANN phylogeny and the impact of gene transfer on archaeal evolution. *Nat Commun* 2020;**11**, DOI: 10.1038/s41467-020-17408-w.

Durante G, Basset A, Stanca E *et al.* Allometric scaling and morphological variation in sinking rate of phytoplankton. *J Phycol* 2019;**55**:1386–93.

Escalas A, Catherine A, Maloufi S *et al.* Drivers and ecological consequences of dominance in periurban phytoplankton communities using networks approaches. *Water Res* 2019;**163**, DOI: 10.1016/j.watres.2019.114893.

Escudié F, Auer L, Bernard M *et al.* FROGS: Find, Rapidly, OTUs with Galaxy Solution. *Bioinformatics* 2018;**34**:1287–94.

Faust K. Open challenges for microbial network construction and analysis. *ISME J* 2021, DOI: 10.1038/s41396-021-01027-4.

Fouilland E, Tolosa I, Bonnet D *et al.* Bacterial carbon dependence on freshly produced phytoplankton exudates under different nutrient availability and grazing pressure conditions in coastal marine waters. *FEMS Microbiol Ecol* 2014;**87**:757–69.

Gaignard C, Laroche C, Pierre G *et al.* Screening of marine microalgae: Investigation of new exopolysaccharide producers. *Algal Res* 2019;**44**, DOI: 10.1016/j.algal.2019.101711.

Gloor GB, Macklaim JM, Pawlowsky-Glahn V *et al.* Microbiome datasets are compositional: And this is not optional. *Front Microbiol* 2017;**8**:1–6.

Goecke F, Thiel V, Wiese J *et al.* Algae as an important environment for bacteria – phylogenetic relationships among new bacterial species isolated from algae. *Phycologia* 2013;**52**:14–24.

Gomes Carvalho Alves KL, Granja-Salcedo YT, Messana JD *et al.* Rumen bacterial diversity in relation to nitrogen retention in beef cattle. *Anaerobe* 2021;**67**, DOI: 10.1016/j.anaerobe.2020.102316.

Grossart HP, Levold F, Allgaier M *et al.* Marine diatom species harbour distinct bacterial communities. *Environ Microbiol* 2005;**7**:860–73.

Guedes IA, Rachid CTCC, Rangel LM *et al.* Close link between harmful cyanobacterial dominance and associated bacterioplankton in a tropical eutrophic reservoir. *Front Microbiol* 2018;**9**, DOI: 10.3389/fmicb.2018.00424.

Hammer Ø, Harper DAT, Ryan PD. Past: Paleontological statistics software package for education and data analysis. *Palaeontol Electron* 2001;**4**:1–9.

Hug LA, Co R. It Takes a Village: Microbial Communities Thrive through Interactions and Metabolic Handoffs. *mSystems* 2018;**3**, DOI: 10.1128/msystems.00152-17.

Hugoni M, Domaizon I, Taib N *et al.* Temporal dynamics of active Archaea in oxygen-depleted zones of two deep lakes. *Environ Microbiol Rep* 2015;**7**:321–9.

Hugoni M, Escalas A, Bernard C *et al.* Spatiotemporal variations in microbial diversity across the three domains of life in a tropical thalassohaline lake (Dziani Dzaha, Mayotte Island). *Mol Ecol* 2018;**27**:4775–86.

Jackrel SL, Yang JW, Schmidt KC *et al.* Host specificity of microbiome assembly and its fitness effects in phytoplankton. *ISME J* 2021;**15**:774–88.

Jurkevitch E, Minz D, Ramati B *et al.* Prey range characterization, ribotyping, and diversity of soil and rhizosphere *Bdellovibrio* spp. isolated on phytopathogenic bacteria. *Appl Environ Microbiol* 2000;**66**:2365–71.

Kharbush JJ, Close HG, Van Mooy BAS *et al.* Particulate Organic Carbon Deconstructed: Molecular and Chemical Composition of Particulate Organic Carbon in the Ocean. *Front Mar Sci* 2020;**7**, DOI: 10.3389/fmars.2020.00518.

Kim G, Bae J, Kim MJ *et al.* The SILVA ribosomal RNA gene database project: Improved data processing and web-based tools. *Nucleic Acids Res* 2019;**41**:1–12.

Kurtz Z, Mueller C, Miraldi E *et al.* SpiecEasi: Sparse inverse Covariance for Ecological Statistical Inference. *R Packag version 106* 2019, DOI: 10.5281/zenodo.3952174.

Kurtz ZD, Müller CL, Miraldi ER *et al.* Sparse and Compositionally Robust Inference of Microbial Ecological Networks. *PLoS Comput Biol* 2015;**11**:1–25.

Leboulanger C, Agogué H, Bernard C *et al.* Microbial diversity and cyanobacterial production in Dziani Dzaha crater lake, a unique tropical thalassohaline environment. *PLoS One* 2017;**12**:1–28.

Lewin RA, Krienitz L, Goericke R *et al. Picocystis salinarum* gen. et sp. nov. (Chlorophyta) - A new picoplanktonic green alga. *Phycologia* 2000;**39**:560–5.

Liang B, Wang LY, Mbadinga SM *et al.* Anaerolineaceae and Methanosaeta turned to be the dominant microorganisms in alkanes-dependent methanogenic culture after long-term of incubation. *AMB Express* 2015;**5**, DOI: 10.1186/s13568-015-0117-4.

Liu H, Roeder K, Wasserman L. Stability approach to regularization selection (StARS) for high dimensional graphical models. *Advances in Neural Information Processing Systems 23: 24th Annual Conference on Neural Information Processing Systems 2010, NIPS 2010*. 2010.

Liu X, Li M, Castelle CJ *et al.* Insights into the ecology, evolution, and metabolism of the widespread Woesearchaeotal lineages. *Microbiome* 2018;**6**, DOI: 10.1186/s40168-018-0488-2.

Liu X, Wang Y, Gu JD. Ecological distribution and potential roles of Woesearchaeota in anaerobic biogeochemical cycling unveiled by genomic analysis. *Comput Struct Biotechnol J* 2021;**19**:794–800.

Mühlenbruch M, Grossart HP, Eigemann F *et al.* Mini-review: Phytoplankton-derived polysaccharides in the marine environment and their interactions with heterotrophic bacteria. *Environ Microbiol* 2018;**20**:2671–85.

Niquil N, Haraldsson M, Sime-Ngando T *et al.* Shifting levels of ecological network's analysis reveals different system properties. *Philos Trans R Soc Lond B Biol Sci* 2020;**375**:20190326.

Nobu MK, Narihiro T, Kuroda K *et al.* Chasing the elusive Euryarchaeota class WSA2: Genomes reveal a uniquely fastidious methyl-reducing methanogen. *ISME J* 2016;**10**:2478–87.

Nolla-Ardevol V, Strous M, Tegetmeyer HE. Anaerobic digestion of the microalga Spirulina at extreme alkaline conditions: Biogas production, metagenome and metatranscriptome. *Front Microbiol* 2015;**6**, DOI: 10.3389/fmicb.2015.00597.

Oksanen J, Blanchet FG, Kindt R *et al.* Vegan: community ecology package. *R Packag version* 2016;**2**.

Pellissier L, Albouy C, Bascompte J *et al.* Comparing species interaction networks along environmental gradients. *Biol Rev* 2018;**93**:785–800.

Pereira S, Zille A, Micheletti E *et al.* Complexity of cyanobacterial exopolysaccharides: Composition, structures, inducing factors and putative genes involved in their biosynthesis and assembly. *FEMS Microbiol Rev* 2009;**33**:917–41.

Phélippé M, Gonçalves O, Thouand G *et al.* Characterization of the polysaccharides chemical diversity of the cyanobacteria *Arthrospira platensis*. *Algal Res* 2019;**38**, DOI: 10.1016/j.algal.2019.101426.

Phillips AA, Speth DR, Miller LG *et al.* Microbial succession and dynamics in meromictic Mono Lake, California. *Geobiology* 2021, DOI: 10.1111/gbi.12437.

Pinhassi J, Sala MM, Havskum H *et al.* Changes in bacterioplankton composition under different phytoplankton regimens. *Appl Environ Microbiol* 2004;**70**:6753–66.

Sarazin G, Jézéquel D, Leboulanger C *et al.* Geochemistry of an endorheic thalassohaline ecosystem: The Dziani Dzaha crater lake (Mayotte Archipelago, Indian Ocean). *Comptes Rendus - Geosci* 2020;**352**:559–77.

Schuurman T, De Boer RF, Kooistra-Smid AMD *et al.* Prospective Study of Use of PCR Amplification and Sequencing of 16S Ribosomal DNA from Cerebrospinal Fluid for Diagnosis of Bacterial Meningitis in a Clinical Setting. *J Clin Microbiol* 2004;**42**:734–40.

Seymour JR, Amin SA, Raina JB *et al.* Zooming in on the phycosphere: The ecological interface for phytoplankton-bacteria relationships. *Nat Microbiol* 2017;**2**, DOI: 10.1038/nmicrobiol.2017.65.

Sunagawa S, Coelho LP, Chaffron S *et al.* Structure and function of the global ocean microbiome. *Science (80-)* 2015;**348**:1261359–1261359.

Tarazona Delgado R, Guarieiro M dos S, Antunes PW *et al.* Effect of nitrogen limitation on growth, biochemical composition, and cell ultrastructure of the microalga *Picocystis salinarum*. *J Appl Phycol* 2021, DOI: 10.1007/s10811-021-02462-8.

Taylor JD, Cottingham SD, Billinge J *et al.* Seasonal microbial community dynamics correlate with phytoplankton-derived polysaccharides in surface coastal waters. *ISME J* 2014;**8**:245–8.

835 Teeling H, Fuchs BM, Bennke CM *et al.* Recurring patterns in bacterioplankton dynamics during coastal
836 spring algae blooms. *Elife* 2016;**5**, DOI: 10.7554/eLife.11888.

837 Tipton L, Müller CL, Kurtz ZD *et al.* Fungi stabilize connectivity in the lung and skin microbial ecosystems.
838 *Microbiome* 2018;**6**, DOI: 10.1186/s40168-017-0393-0.

839 Trabelsi L, Ben Ouada H, Bacha H *et al.* Combined effect of temperature and light intensity on growth and
840 extracellular polymeric substance production by the cyanobacterium *Arthrospira platensis*. *J Appl*
841 *Phycol* 2009;**21**:405–12.

842 Troussellier M, Escalas A, Bouvier T *et al.* Sustaining rare marine microorganisms: Macroorganisms as
843 repositories and dispersal agents of microbial diversity. *Front Microbiol* 2017;**8**:1–17.

844 Ventosa A, de la Haba RR, Sánchez-Porro C *et al.* Microbial diversity of hypersaline environments: A
845 metagenomic approach. *Curr Opin Microbiol* 2015;**25**:80–7.

846 Wagg C, Schlaeppi K, Banerjee S *et al.* Fungal-bacterial diversity and microbiome complexity predict
847 ecosystem functioning. *Nat Commun* 2019;**10**:1–10.

848 Walters W, Hyde ER, Berg-Lyons D *et al.* Improved Bacterial 16S rRNA Gene (V4 and V4-5) and Fungal
849 Internal Transcribed Spacer Marker Gene Primers for Microbial Community Surveys. *mSystems*
850 2016;**1**, DOI: 10.1128/msystems.00009-15.

851 De Wit R, Bouvier T. "Everything is everywhere, but, the environment selects"; what did Baas Becking and
852 Beijerinck really say? *Environ Microbiol* 2006;**8**:755–8.

853 Xiao R, Yang X, Li M *et al.* Investigation of composition, structure and bioactivity of extracellular polymeric
854 substances from original and stress-induced strains of *Thraustochytrium striatum*. *Carbohydr Polym*
855 2018;**195**:515–24.
856
857
858
859
860
861
862
863

Table 1: Environmental conditions in the two environmental niches observed in Lake Dziani Dzaha

Differences between the two niches were tested using Wilcoxon rank sum test and the p-values were adjusted using the Bonferroni correction. Presented values are mean±sd. Wilcoxon rank sum test: *** : p values < 0.001, ** : pvalue < 0.01, * : pvalue < 0.05.

	Surface	Bottom	
Temperature (°C)	30.88 ± 1.09	30.00 ± 0.25	
pH	9.33 ± 0.30	9.12 ± 0.24	
O_2 (% saturation)	79.16 ± 128.74	0.38 ± 0.75	
Salinity (psu)	55.71 ± 12.25	66.34 ± 3.19	***
Eh (mV)	-53.63 ± 147.46	-324.41 ± 56.81	***
H_2S/HS^- ($\mu mol.L^{-1}$)	99.79 ± 100.90	3051.58 ± 1962.88	***
Chl a ($\mu g.L^{-1}$)	556.34 ± 168.50	206.80 ± 143.53	***

Table 2: Comparison of the composition and structure of microbial communities from the two environmental niches observed in Lake Dziani Dzaha

Differences between the two niches were tested PERMANOVA.

		Composition (Jaccard)					Structure (Bray-Curtis)				
	Df	MeanSqs	F	R^2	p-value		MeanSqs	F	R^2	p-value	
All domains	1	1.44	10.96	0.30	0.001	***	1.09	15.87	0.38	0.001	***
	26	0.13	-	0.70	-		0.07	-	0.62	-	
Archaea	1	1.55	9.21	0.26	0.001	***	1.23	12.78	0.33	0.001	***
	26	0.17	-	0.74	-		0.10	-	0.67	-	
Bacteria	1	1.73	11.55	0.31	0.001	***	1.50	16.60	0.39	0.001	***
	26	0.15	-	0.69	-		0.09	-	0.61	-	
Eukaryota	1	0.13	2.93	0.10	0.025	*	0.05	2.98	0.10	0.03	*
	26	0.05	-	0.90	-		0.02	-	0.90	-	

Table 3: Comparison of global networks characteristics

Average metrics values estimated across networks from each niche. Wilcoxon rank sum test: *** : p values < 0.001, ** : pvalue < 0.01, * : pvalue < 0.05.

	Niche		t-test		
Network characteristic	**Surface**	**Bottom**	**t**	**p-value**	
Number of nodes	272	310	3.2	0.004	**
Number of links	790	1099	5.1	0.000	***
Network diameter	8.5	6.9	-5.0	0.000	***
Network density	2.9	3.5	7.2	0.000	***
Average inter-node distance	3.8	3.4	-6.4	0.000	***
Centralized degree	1641	1893	2.3	0.032	*
Centralized betweenness	253668	246414	-0.5	0.648	
Centralized closeness	13.7	14.1	0.5	0.624	
Hub score	43.5	65.3	9.4	0.000	***

Table 4: Direct association of dominant taxa in both niches

Dominant taxa	Niche	Linked OTU	Domain	Phylum	Class	Order	Family	Link type
A. fusiformis								
	Surface	Bac_OTU_14	Bacteria	Bacteroidetes	Bacteroidia	Bacteroidales	ML635J-40aquaticgroup	Negative
		Bac_OTU_44	Bacteria	Bacteroidetes	Bacteroidia	Bacteroidales	ML635J-40aquaticgroup	Negative
		Bac_OTU_69	Bacteria	Deinococcus-Thermus	Deinococci	Deinococcales	Trueperaceae	Positive
		Bac_OTU_179	Bacteria	Firmicutes	Clostridia	Clostridiales	Syntrophomonadaceae	Negative
		Bac_OTU_307	Bacteria	Firmicutes	Clostridia	Halanaerobiales	ODP1230B8.23	Positive
		Arc_OTU_8	Archaea	Woesearchaeota(DHVEG-6)	Uknown class	Uknown order	Uknown family	Positive
		Arc_OTU_61	Archaea	Woesearchaeota(DHVEG-6)	Uknown class	Uknown order	Uknown family	Negative
	Bottom	Bac_OTU_29	Bacteria	Bacteroidetes	Bacteroidia	Bacteroidales	ML635J-40aquaticgroup	Negative
		Bac_OTU_32	Bacteria	Bacteroidetes	Bacteroidia	Bacteroidales	ML635J-40aquaticgroup	Negative
		Bac_OTU_127	Bacteria	Bacteroidetes	Bacteroidia	Bacteroidales	ML635J-40aquaticgroup	Negative
		Bac_OTU_130	Bacteria	Bacteroidetes	Bacteroidia	Bacteroidales	ML635J-40aquaticgroup	Negative
		Bac_OTU_195	Bacteria	Elusimicrobia	Elusimicrobia	Rs-M47	Uknown family	Negative
		Bac_OTU_196	Bacteria	Firmicutes	Clostridia	Halanaerobiales	ODP1230B8.23	Negative
		Bac_OTU_199	Bacteria	Proteobacteria	Alphaproteobacteria	Rhodospirillales	Rhodospirillaceae	Positive
		Bac_OTU_201	Bacteria	Proteobacteria	Alphaproteobacteria	Rhodobacterales	Rhodobacteraceae	Positive
		Bac_OTU_271	Bacteria	Firmicutes	Clostridia	Clostridiales	Syntrophomonadaceae	Negative
P. salinarum								
	Surface	Bac_OTU_11	Bacteria	Bacteroidetes	Sphingobacteriia	Sphingobacteriales	Lentimicrobiaceae	Negative
		Bac_OTU_189	Bacteria	Bacteroidetes	Bacteroidia	Bacteroidales	ML635J-40aquaticgroup	Positive
		Bac_OTU_237	Bacteria	Bacteroidetes	BacteroidetesIncertaeSedis	OrderIII	ML310M-34	Negative
		Arc_OTU_50	Archaea	Euryarchaeota	Methanomicrobia	Methanosarcinales	Methanosarcinaceae	Positive
		Arc_OTU_81	Archaea	Euryarchaeota	Thermoplasmata	Thermoplasmatales	MarineBenthicGroupDandDHVEG-1	Positive
		Arc_OTU_107	Archaea	Bathyarchaeota	Uknown class	Uknown order	Uknown family	Positive
		Euk_OTU_149	Eukaryota	Ciliophora	Intramacronucleata	Spirotrichea	Hypotrichia	Negative
	Bottom	Bac_OTU_73	Bacteria	Actinobacteria	Nitriliruptoria	Euzebyales	Euzebyaceae	Positive
		Bac_OTU_77	Bacteria	Firmicutes	Clostridia	M55-D21	Uknown family	Positive
		Bac_OTU_169	Bacteria	Firmicutes	Clostridia	Clostridiales	Syntrophomonadaceae	Positive
		Bac_OTU_264	Bacteria	Synergistetes	Synergistia	Synergistales	Synergistaceae	Positive
		Arc_OTU_116	Archaea	Woesearchaeota(DHVEG-6)	Uknown class	Uknown order	Uknown family	Positive
		Euk_OTU_3	Eukaryota	Ancyromonadida	Uknown class	Uknown order	Uknown family	Negative
		Euk_OTU_45	Eukaryota	Stramenopile	Placididea	Uknown order	Uknown family	Positive

Figure 1: Delineation of two contrasted ecological zones in the Dziani Dzaha lake

A: Physico-chemical characteristics of the studied samples. Diamonds and circles correspond to stratified and unstratified seasons, respectively, while filled and empty dots correspond to 2014 and 2015 surveys, respectively. For each variable the samples are colored according to the ecological zone they belong to (surface or bottom cluster in B).

B: Dendrogram representing the separation of samples in two clusters, based on euclidean distance between samples computed using the seven variables presented in A.

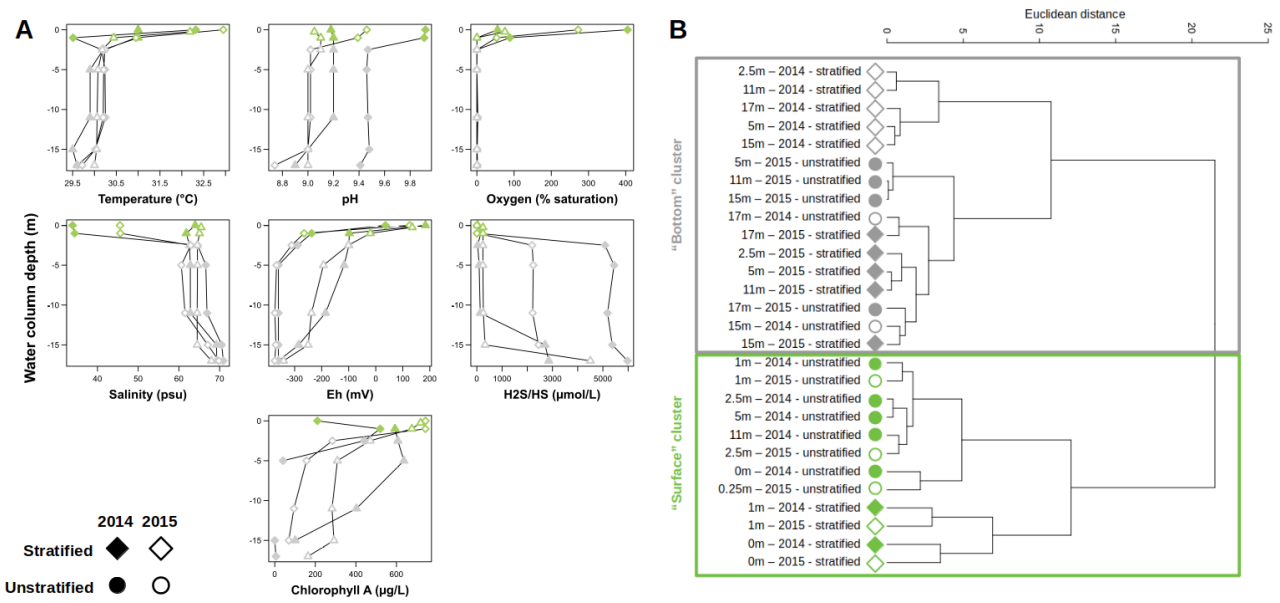

Figure 2: Global characteristics of association networks in each environmental niche

Each boxplot represents the distribution of values observed across the networks from each separated community (n = 12 and 16 for surface and bottom, respectively). The p-values of the Wilcoxon rank sum test comparing the two niches are presented below each subplot.

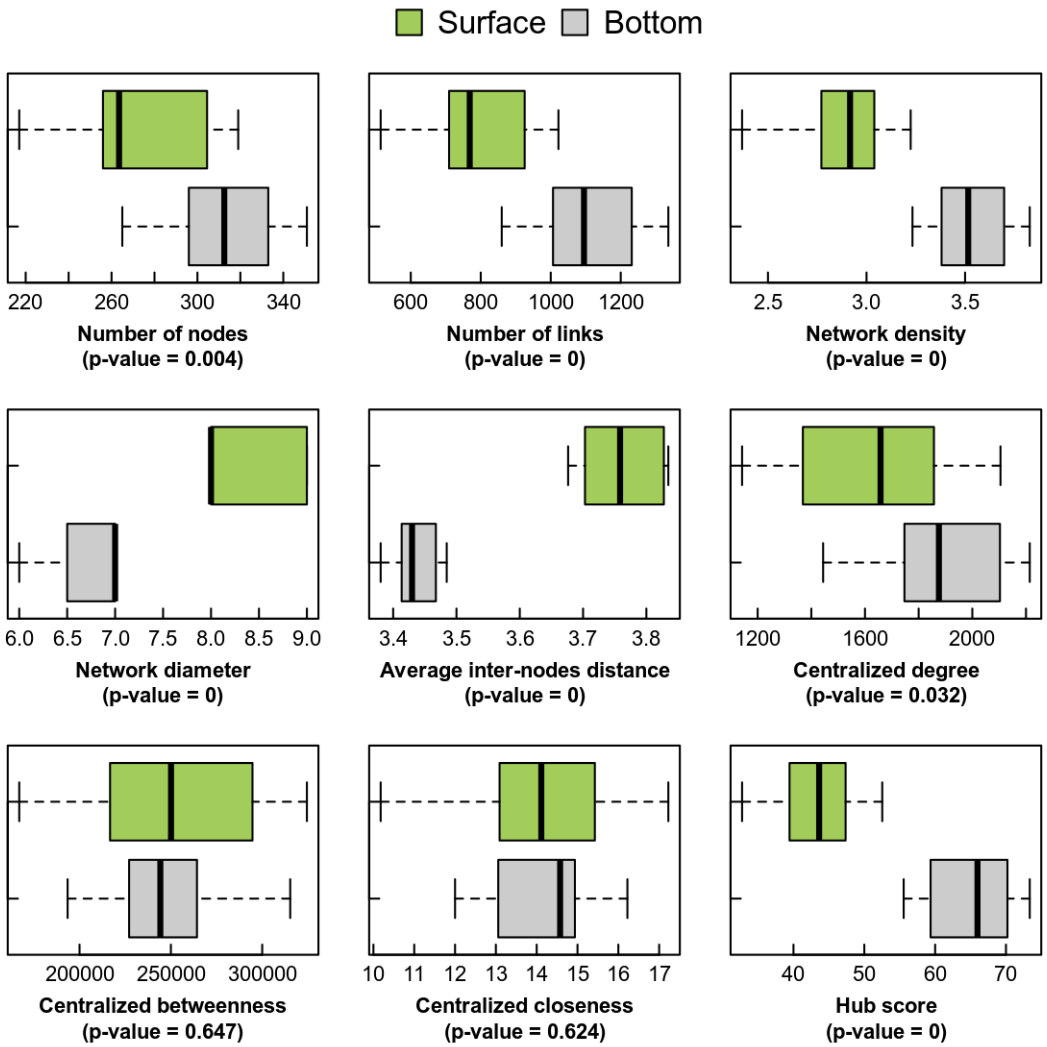

Figure 3: Taxonomic composition of modules in both niches

This figure corresponds to the modules identified using the walktrap clustering algorithm. Archaea phyla are in nuances of red, Bacteria in nuances of blue and Eukaryota in nuances of brown. *A. fusiformis* was detected in modules S_11 and B_9 while *P. salinarum* was detected in modules S_5 and B_

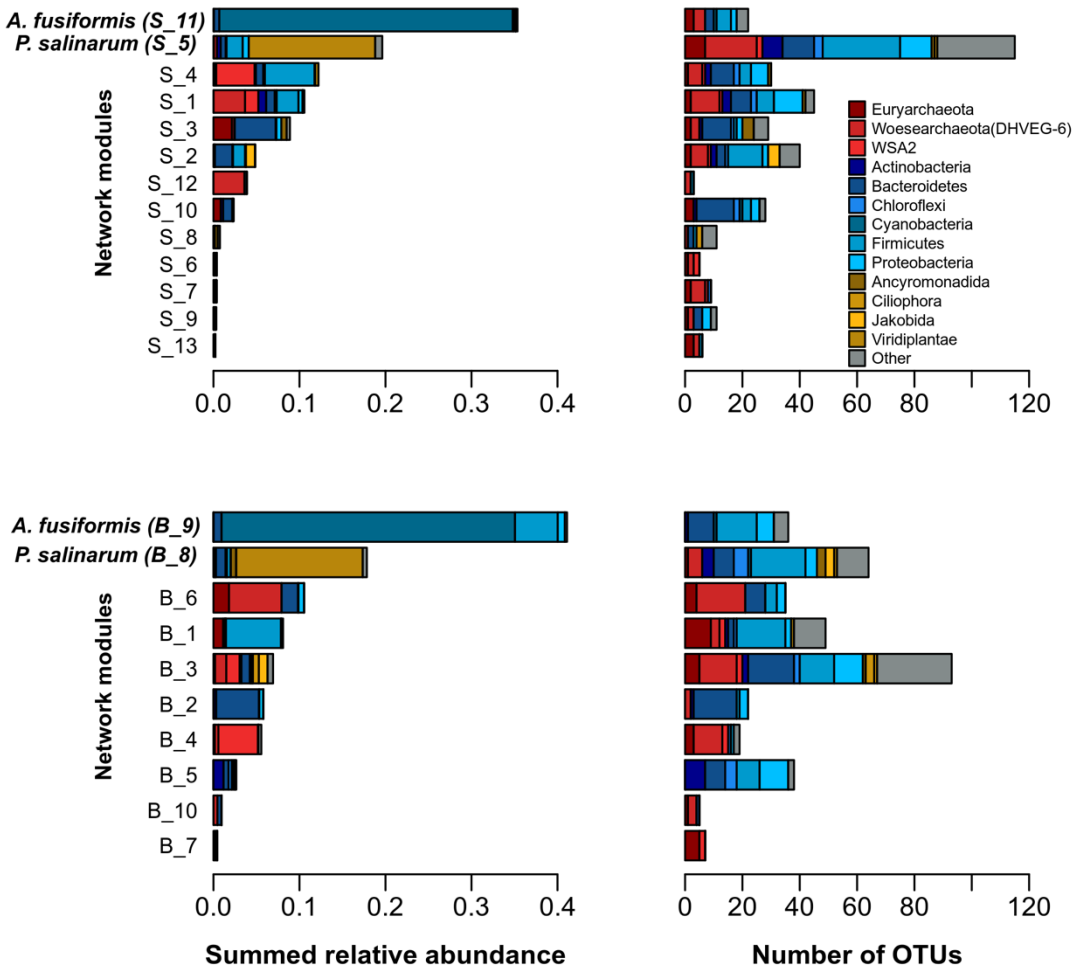

Figure 4: Taxonomy of peripheral and central nodes in both niches

Peripheral and central nodes (*i.e.* OTUs) were identified as the one with an average centrality rank falling within the first and tenth decile, respectively (cf. Figure S6, n = 36 and 37 in surface and bottom niches, respectively). Top plot corresponds to taxonomic classification at the Domain level while bottom plot corresponds to Phylum level.

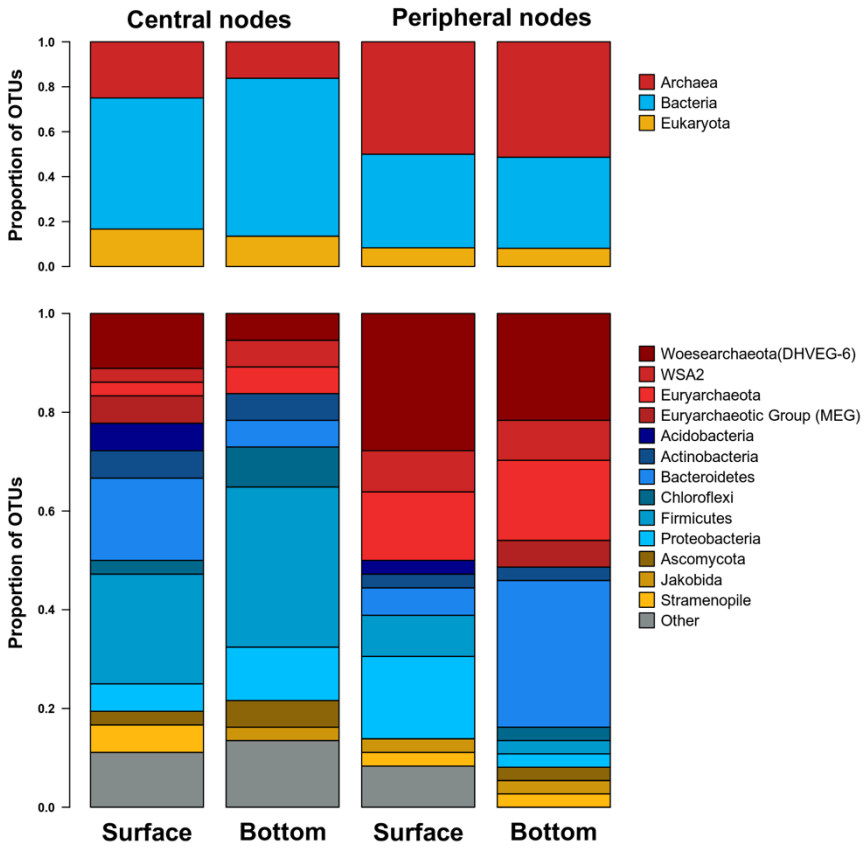

Figure 5: Conceptual model of the functioning of Lake Dziani Dzaha ecosystem
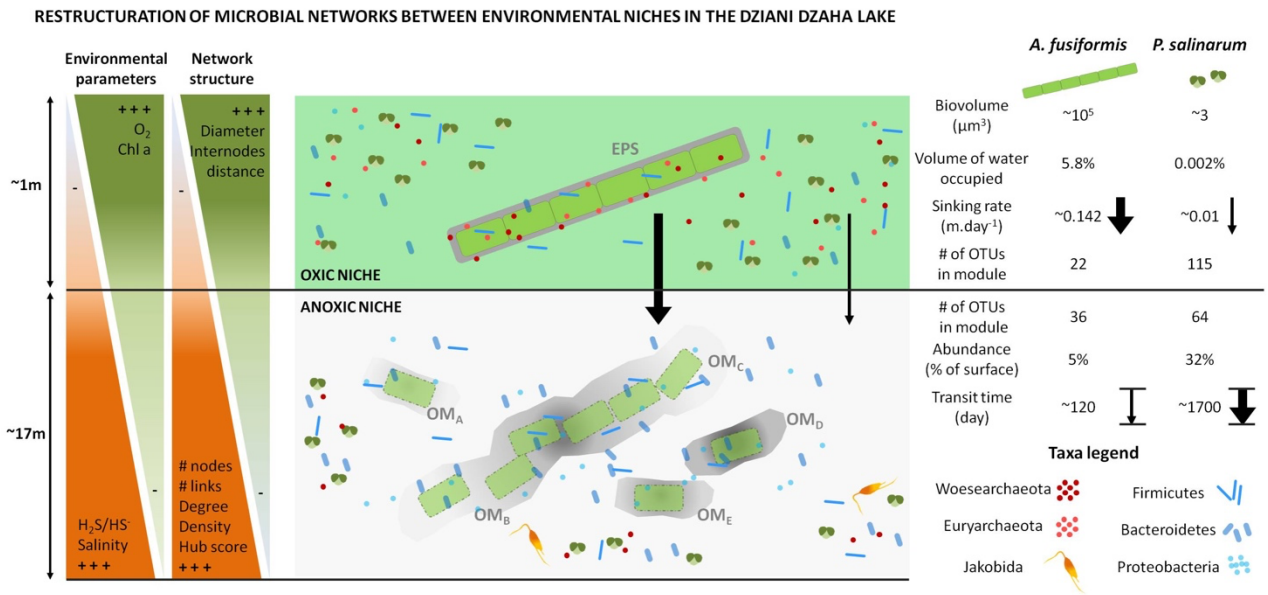
This figure presents a conceptual model of the Lake Dziani Dzaha functioning, centered around the two main primary producers. The left part of the figure represents the change in environmental parameters and network characteristics between the two niches. The right part represents the characteristics of the two main primary producers. The central part represents the spatial organization of the primary producers and of the main taxonomic groups in both niches. The decomposition of *A. fusiformis* and its surrounding exopolysaccharides (EPS) into different organic matter pools (OM) is figured with the shading of the EPS matrix around lyzed cells.